IEEE Access
Multidisciplinary | Rapid Review | Open Access Journal

Date of publication xxxx 00, 0000, date of current version xxxx 00, 0000.

Digital Object Identifier 10.1109/ACCESS.2017.DOI

Real-World Performance of Sub-1 GHz and 2.4 GHz Textile Antennas for RF-Powered Body Area Networks

Mahmoud Wagih, (Graduate Student Member, IEEE), Oktay Cetinkaya, (Member, IEEE), Bahareh Zaghari, (Member, IEEE), Alex S. Weddell, (Member, IEEE), and Steve Beeby, (Senior Member, IEEE)

School of Electronics and Computer Science, University of Southampton, Southampton, SO17 1BJ UK (email. mahm1g15@ecs.soton.ac.uk)

Corresponding author: Mahmoud Wagih (e-mail: mahm1g15@ecs.soton.ac.uk).

This work was supported by the UK Engineering and Physical Sciences Research Council (EPSRC) under Grant EP/P010164/1 and the European Commission through the EnABLES Project funded under H2020-EU.1.4.1.2. Grant number 730957
Datasets supporting this article are available from the University of Southampton Repository at DOI: 10.5258/SOTON/D1479.

ABSTRACT In Radio Frequency (RF)-powered networks, peak antenna gains and path-loss models are often used to predict the power that can be received by a rectenna. However, this leads to significant over-estimation of the harvested power when using rectennas in a dynamic setting. This work proposes more realistic parameters for evaluating RF-powered Body Area Networks (BANs), and utilizes them to analyze and compare the performance of an RF-powered BAN based on 915 MHz and 2.4 GHz rectennas. Two fully-textile antennas: a 915 MHz monopole and a 2.4 GHz patch, are designed and fabricated for numerical radiation pattern analysis and practical forward transmission measurements. The antennas' radiation properties are used to calculate the power delivered to a wireless-powered BAN formed of four antennas at different body positions. The mean angular gain is proposed as a more insightful metric for evaluating RFEH networks with unknown transmitter-receiver alignment. It is concluded that, when considering the mean gain, an RF-powered BAN using an omnidirectional 915 MHz antenna outperforms a 2.4 GHz BAN with higher-gain antenna, despite lack of shielding, by 15.4× higher DC power. Furthermore, a transmitter located above the user can result in 1× and 9× higher DC power at 915 MHz and 2.4 GHz, respectively, compared to a horizontal transmitter. Finally, it is suggested that the mean and angular gain should be considered instead of the peak gain. This accounts for the antennas' angular misalignment resulting from the receiver's mobility, which can vary the received power by an order of magnitude.

INDEX TERMS Antennas, Body Area Networks (BAN), Electronic Textiles, Energy Harvesting, Internet of Things, ISM Bands, RF Energy Harvesting, Wearable Antenna, Wireless Power Transfer

I. INTRODUCTION

TEXTILE-BASED and wearable antennas [1], sensor nodes [2], energy harvesters [3] and Wireless Power Transfer (WPT) modules [4] have been proposed to enable reliable and autonomous Body Area Networks (BANs) on flexible and wearable materials for seamless integration in garments. BANs and body-centric passive sensing have various interesting applications in a smart city environment, such as tracking diabetic patients [5]. For active wearable sensing and communication nodes, power-autonomy is a fundamental need for the Internet of Things (IoT) [6], [7].

WPT and Radio Frequency Energy Harvesting (RFEH) are methods of enabling power-autonomous networking [8], and are considered as a controllable power harvesting and transfer technique for powering the IoT [9]. Antennas and coils for WPT on textile substrates using flexible materials have been widely-reported [4], [10]. Rectifying antennas (rectennas) are the main energy harvesting component, where the received power from the dedicated WPT or ambient RFEH source is dependent on the antenna's parameters such as gain, beamwidth, and polarization [11]. Such antenna parameters are highly angle-dependent and hence will vary with the source-rectenna alignment. While the peak gain is introduced as a figure of merit in link-budget calculations in WPT [12], in an ambient RFEH environment using a more directional antenna does not translate to higher energy reception [13],

where the direction of the incident power may not align with the narrower beam-width.

Wireless networks powered through RFEH or WPT from a dedicated wireless power base-station have been extensively studied [14]. In addition, Simultaneous Wireless Information and Power Transfer (SWIPT) has been proposed utilizing the same carrier frequency to power a battery-less receiver while decoding the information carried by the RF wave [15]. Power transfer using digitally-modulated wave-forms has been studied for SWIPT applications based on off-the-shelf energy harvesters [16]. SWIPT has previously been utilized in back-scattered RFID [17]. Moreover, wireless powering of implants has been demonstrated using radiative Ultra-High Frequency (UHF) WPT [18], [19].

To enable RF-powering of e-textiles and BANs, textile-based rectennas and antennas have been realized using various fabrication methods and frequency bands from sub-1 GHz UHF up to mmWave bands [10], [20]–[24]. Wearable rectenna designs have been focused on antenna designs shielded from the body and hence utilize patch antennas. Recently, an unshielded tee-shirt rectenna array has been proposed for broadband applications [25]. To overcome the efficiency degradation due to human proximity, a large array (9×9) is used to improve the power received by the rectenna.

The trade-offs in RF-powered network design include the choice of the carrier frequency, transmitter and receiver antenna designs and therefore the gain [11], and the nodes distribution [26]. For instance, it has been shown that the energy coverage is improved in the 28 GHz mmWave band compared to sub-6 GHz networks due to the highly-directional large antenna arrays at mmWave bands [27]. However, realizing high-efficiency rectifiers at such a high frequency is difficult due to the diodes' cut-off frequencies. On the other hand, a sub-1 GHz carrier allows the reduction of the propagation losses and the use of existing transmitters such as RFID readers [17]. RF-powering using drones [28], fixed energy harvesting base-stations [29], and ray-tracing [30] have been reported demonstrating the possibility of powering multiple nodes reliably using RF power. While a standard (non-textile) rectenna has been evaluated using the 3D voltage radiation patterns [31], most textile-based rectennas have been characterized using standard antenna parameters such as the peak gain and radiation efficiency. On the other hand, the layout of the rectifier and the feeding mechanism of the rectenna may distort the radiation patterns of the characterized antenna-only prototype

RF propagation in on- and off-body scenarios has been widely investigated for different frequency bands [32], [33]. Recent work has focused on maximizing the efficiency of an on-body link using fixed antennas, where the path loss could be minimized using beam-steering or directional antennas [32]. Wireless links for in-body wearable communications have been investigated for UWB implants [34]. However, most on-body propagation studies are concerned with fixed antennas, where the only variation may be introduced by the movement of certain body parts. When it comes to an RFEH or WPT scenario, the angle of incidence of the RF power may not be aligned with the rectenna's main-beam. Furthermore, while an antenna radiating off-body, such as a microstrip patch, has been favorable for wearable rectennas [10], [22], [23], it may significantly reduce the power received from a transmitter shadowed by the body. This is due to the antenna's high front-to-back ratio, requiring more rectennas with additional techniques for DC-combining, to achieve the same angular coverage which may reduce the efficiency compared to a single rectenna [23].

This work evaluates the performance of an RF-powered BAN at two different license-free Industrial Scientific Medical (ISM) bands, 915 MHz and 2.4 GHz, using fully-textile antennas, i.e. antennas with textile conductors such as Litz threads [4], and electroplated fabrics [10]. A 915 MHz monopole and a 2.4 GHz patch are designed, simulated on a human model, and fabricated. The antenna prototypes are utilized for off-body path loss measurements and compared to reference dipole antennas positioned in free space. A BAN powered using four rectennas based on the characterized textile antennas is evaluated to identify the frequency band and antenna design resulting in the highest DC power reception.

The contributions of this paper can be summarized in:

1) Proposing the mean (average) angular gain and angular gain probability as metrics for evaluating energy harvesting antennas for mobile receivers such as wearable rectennas.
2) Numerically and experimentally comparing the LOS and N-LOS off-body "effective gain" of 915 MHz omnidirectional and 2.4 GHz broadside textile antennas.
3) Evaluating the performance of a 915 MHz and 2.4 GHz BAN based on multiple wearable rectennas using the angular mean gain and the gain distribution function.
4) Demonstrating that a 915 MHz unshielded antenna is more suited for ISM-band WPT compared to a 2.4 GHz patch with a potential for up to $15\times$ higher DC power reception.

This paper is structured as follows: section II presents the architecture of the BAN studied in this work. The textile antennas used in this study are designed and characterized in section III, the antennas are then used in section IV to measure the off-body propagation losses. Finally, the power received by a BAN powered using the designed textile antennas is evaluated in section V.

II. BODY AREA NETWORK ARCHITECTURE

In a wearable RFEH-BAN, it is expected that multiple nodes integrated in the user's garment can be wireless-powered using an off-body source. In this context, "off-body" radiation is defined as incident electromagnetic (EM) radiation from an antenna placed off the body. "On-body" propagation between two wearable antennas integrated in the same user's clothing is not considered in this study, as the power is delivered from an off-body transmitter. Scalable integration of rectennas in textiles and garments have previously been reported in a double-sided wrist bands, [23], to overcome

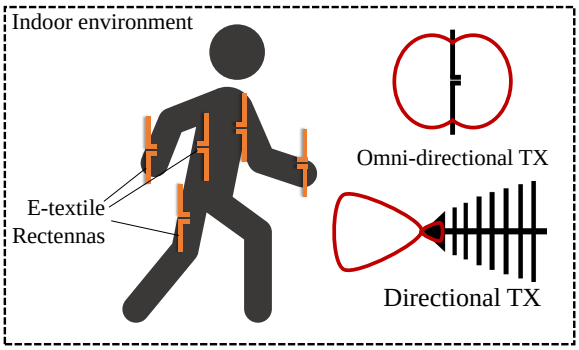

FIGURE 1. A wireless-powered BAN, powered using directional or omnidirectional dedicated license-free transmitters.

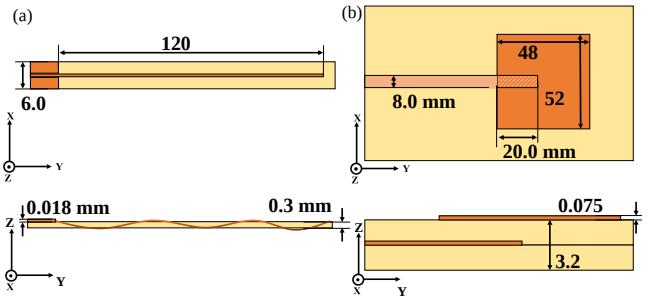

FIGURE 2. Layout and dimensions of the proposed textile AUTs: (a) 915 MHz monopole, (b) 2.4 GHz patch.

the directionality problem when the harvesting patch is not facing the transmitter. In addition, a 4×2 patch antenna array has been proposed to improve the DC power received from an incident plane-wave excitation [22].

In this paper, a BAN with multiple rectennas is considered; the power received by the rectennas is combined into a single DC output. The rectennas will be powered using a UHF license-free transmitter operating at either 915 MHz or 2.4 GHz. In an indoor environment, the rectenna's efficient harvesting range may not exceed 5 m due to the limits on the Equivalent Isotropically Radiated Power (EIRP) [35]. Therefore, the impact of the antenna's radiation properties, i.e. gain and angular beamwidth, will have significant impact on the received RF and subsequently DC power. Moreover, the position of the transmitter with respect to the user needs to be considered as an additional tuning parameter. For example, a transmitter at the same height as the user (horizontal), as opposed to a transmitter above the user (vertical) will affect the power received by the rectenna. The effects of the antennas' radiation properties for wearable RFEH need to be based on the radiation patterns of realistic fully-textile antennas in different RFEH scenarios, such as Line-of-Sight (LOS) and non-LOS operation. Fig. 1 shows a BAN powered using off-body transmitters at license-free bands.

III. WEARABLE ENERGY HARVESTING ANTENNA

A. ANTENNA DESIGN

To investigate the off-body propagation and radiation properties, and hence evaluate the harvesting capabilities of wearable rectennas, two antenna designs are proposed. The antennas are designed for a standard textile substrate and are fabricated using conductive threads and electroplated e-textiles. Thus, the measured performance of these antennas will be indicative of textile-based rectenna performance in wearable applications.

At sub-1 GHz bands, unshielded textile antennas may be used to maintain a low profile [36]. To explain, the relatively long wavelength (32.8 cm at 915 MHz) implies that a ground plane or an unconnected reflector will need to be placed over 1 cm behind the antenna to prevent detuning, which is unrealistic in a planar textile antenna. Therefore, textile antennas operating at sub-1 GHz have been considered with varying textile separation layers [37] as well as with variable separation from the human body [38], to investigate the impact on their radiation efficiency and gain.

The proposed antenna for sub-1 GHz WPT is a textile wire monopole, sewn using a conductive thread onto a standard (poly-cotton) textile substrate. Such a monopole antenna will have a lower gain than a dipole's theoretical directivity of 2.1 dBi [39]. This is due to the compact ground plane and the additional conductor losses in the textile Litz wire. Fig. 2-a shows the dimensions of the monopole microstrip antenna.

At 2.4 GHz, implementing a ground-backed patch antenna on textiles with reasonable (above 10%) radiation efficiency is more feasible. For example, the rectennas reported in [22] and [23] utilized patch antennas on textiles with up to 76% measured radiation efficiency in [23]. Fig. 2-b shows the dimensions of the patch antenna considered in this work. Fig. 3 shows the photographs of the textile antenna prototypes. Both antennas utilize highly conductive textiles (sheet resistance$<$10 mΩ/square) and therefore the fabrication techniques and materials will introduce minimum variation in the antennas' efficiency and gain compared to state-of-the-art textile antennas.

B. ANTENNA SIMULATION AND MEASUREMENTS

The antennas have been simulated using full-wave 3D EM simulation in CST Microwave Studio. The dielectric properties of the substrates used were based on the measured properties of felt and polyester cotton reported in [23]. The fabricated prototypes were connected to standard solder-terminated SMA connectors and their bandwidth was measured using a Vector Network Analyser (VNA).

The measured reflection coefficient (S_{11}) of the monopole and patch antennas in Fig. 4 shows a $S_{11} < -10$ dB bandwidth at 915 MHz and 2.45 GHz respectively. Thus, they can be used to measure the off-body propagation at these bands without any influence on the realized gain. The main discrepancy in the monopoles' S_{11} magnitude is due to the ground plane's size resulting in a more capacitive antenna in simulation. On the other hand, the SMA connector increases the actual ground plane size of the antenna during measurements resulting in the improved impedance match.

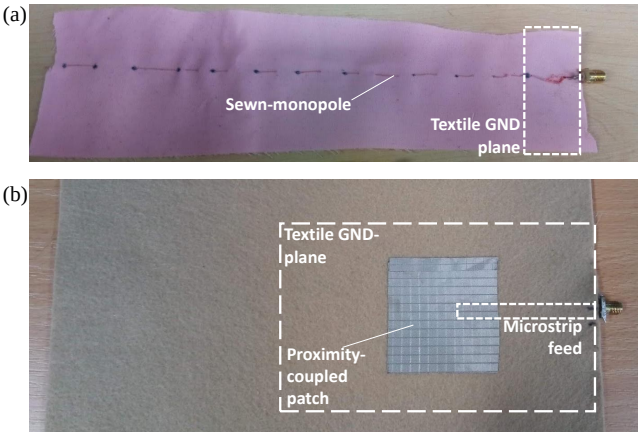

FIGURE 3. Photographs of the textile antennas used in the channel measurements: 915 MHz sewn monopole (a) and 2.4 GHz conductive fabric patch (b).

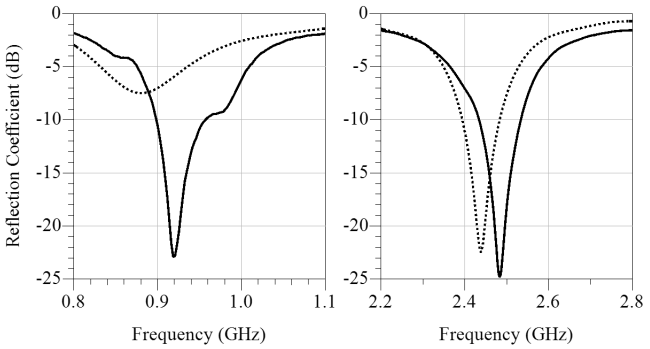

FIGURE 4. Simulated (dashed) and measured (solid) reflection coefficient of the textile monopole (left) and patch (right) antennas utilized in the off-body propagation measurements.

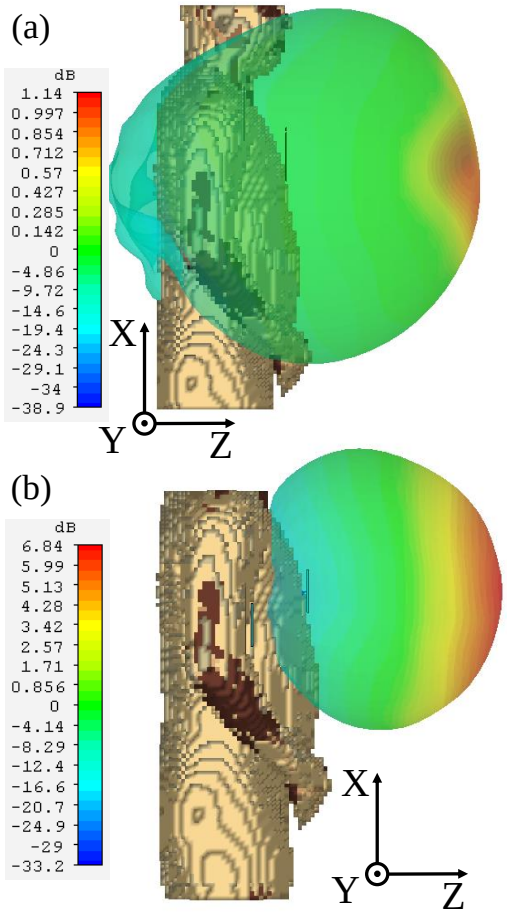

FIGURE 5. Simulated 3D farfield gain radiation patterns of the 915 MHz monopole (a) and the 2.4 GHz patch antenna (b).

C. OFF-BODY ANTENNA NEAR AND FAR-FIELDS

Field monitors in CST Microwave Studio have been used to investigate the near and far-field distributions around the human body. The EM-simulated radiation patterns will be utilized to analytically evaluate the performance of the network in Section V. The open-source human body EM simulation model AustinMan, [40], has been used to simulate the antenna's performance in proximity with the human body. The model utilized in this work is detailed to $8\times8\times8$ mm^3, as this work only considers off-body antenna and not implants in specific body positions, this resolution satisfies the accuracy requirement for a reasonable computation time and solver mesh size.

Two on-body antenna positions, on-chest and on-arm, have been considered to evaluate the radiation properties and mutual coupling between the antennas. To simplify the 3D modeling and reduce the time-domain solver mesh size, the antennas have been considered in a flat state, reducing the number of cells required to simulate the antenna. Textile-based patch antennas have previously been studied under bending and did not show variation around their resonant frequency [23]. The antennas have been placed at 5 mm clearance from the skin layer on the AustinMan phantom. The on-chest 915 MHz monopole antenna achieves a 1.1 dB gain with 3 dB beamwidth of 95°, while the 2.4 GHz patch achieves a gain of 6.84 dB with a narrower 63.7° 3 dB-beamwidth. The simulated 3D radiation patterns of the monopole and patch antennas are shown in Fig. 5-a and 5-b, respectively.

The near-field electric- (E-) field patterns around the antennas have been simulated to visualize the mutual-coupling between the wearable antennas. Fig. 6-a and -b show the E-field radiated from the 915 MHz textile monopole on-chest and on-shoulder. The e-field of the 2.4 GHz patches is shown in Fig. 7. It is observed that from both antennas, less than 1% of the radiated E-field is received by the other antenna. This has been validated by the S_{21} being less than -30 and -40 dB for the monopole and patch antennas, respectively, when placed on-chest and on-shoulder.

Near-field plots allow visualizing and understanding antennas' interaction with the human body [2]. This can be used to evaluate and understand the impact of different body positions on the power radiate by the antenna. Therefore, the E-field patterns of the the transmitting antenna can be used to understand the interaction of an incident wave on a receiver

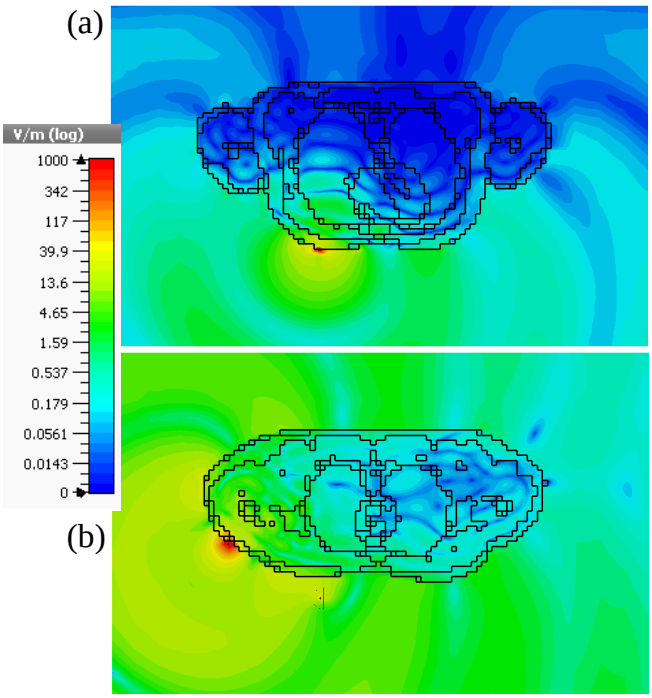

FIGURE 6. Simulated E-field distribution around the body at 915 MHz from: (a) antenna placed on the chest, (b) antenna placed on shoulder

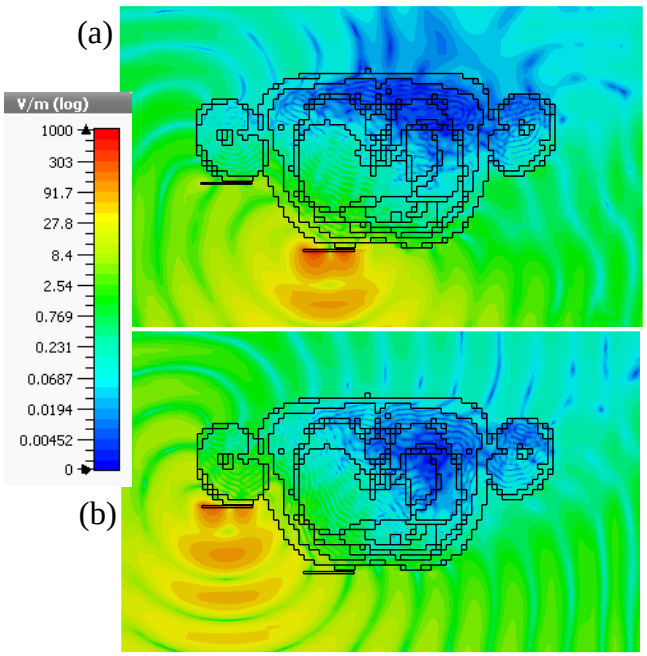

FIGURE 7. Simulated E-field distribution at 2.4 GHz from: (a) patch antenna on-chest, (b) patch antenna on shoulder.

with the body, due to reciprocity. For example, the on-shoulder antenna in Fig. 6-b shows the antenna's near-field surrounding the body with minimal body-shadowing effects. Hence, it is suggested to place off-body WPT antennas on the body's extremities to minimize shadowing. Furthermore, in Fig. 6-b, the E-field magnitude behind the user is higher than that of the patch in Fig. 7-b. This indicates the monopole antenna's ability to receive more power when not facing the transmitter compared to the patch, despite suffering from increased absorption and shielding by the body, due to its own lack of a metal plane or a reflector.

IV. OFF-BODY PROPAGATION MEASUREMENTS

To evaluate the performance of wearable RFEH antennas operating on the body, the textile antennas shown in Fig. 3 were used to measure the propagation losses between a directional transmitter and the wearable antenna. A reference wire-dipole antenna (of ideal 2.1 dB gain) has also been used at 915 MHz for benchmarking. A standard 10 dBi log-periodic antenna has been utilized as a fixed transmitter horizontal to the user. A VNA has been used to measure the Continuous Wave (CW) forward transmission (S_{21}) between the antenna-under-test (AUT) and the 10 dBi reference. The measurements were performed on a standing person, and do not include the effects of walking on the path loss. Fig. 8 shows the measurement setup.

The antennas were placed at a fixed distance D and the S_{21} between the source and the AUT has been measured. D has been set to 1 m from the radiating apertures of the transmitting and receiving antennas to ensure operation in the far-field region of the AUTs.

The antennas have been placed on multiple on-body positions, shown in Fig. 8-a, to accurately measure the impact of different body parts on the antenna's effective gain. The effective gain,

$$G_{\text{eff}} = S_{21\ \text{textile}} - S_{21\ \text{dipole}}, \tag{1}$$

is introduced to factor in the body shadowing effects compared to the S_{21} of an ideal 2.1 dBi $\lambda/2$ wire dipole measured in free space at the same D. This eliminates the errors due to multi-path effects and due to uncertainties in the path loss model or the transmitter gain. G_{eff} differs from standard gain measurements on a human body phantom by combining the off-body propagation effects in the gain figure. For instance, in the N-LOS case, the human body is a main contributor to the lower G_{eff}, due to shadowing. G_{eff} in the N-LOS case of a broadside patch antenna is reduced both by the body-shadowing effect as well as the antenna's own main beam misalignment with the transmitter. G_{eff} is relative to the dipole's gain.

The measured channel losses have been used to calculate the effective gain of the antennas shown in Table IV. By observation, the effects of LOS and N-LOS off-body propagation can be accounted for using the antenna's gain. Therefore, the propagation model can be simplified to free-space propagation. In addition, by performing the G_{eff} measurements on-body in an indoor environment, this factors in additional multi-path effects and the effects of clothing.

When comparing the unshielded 915 MHz omni-directional with the 2.4 GHz broad-side patch antenna, as predicted, the patch antenna maintains a higher effective gain

TABLE 1. Measured off-body effective gain (G_{eff}) of the AUTs

Body Pos.	3 cm from body: LOS			3 cm from body: N-LOS			Body contact: LOS			Body contact: N-LOS		
	Ref. dipole	Textile monopole	Textile patch	Ref. dipole	Textile monopole	Textile patch	Ref. dipole	Textile monopole	Textile patch	Ref. dipole	Textile monopole	Textile patch
	915 MHz		2.4 GHz	915 MHz		2.4 GHz	915 MHz		2.4 GHz	915 MHz		2.4 GHz
I	-2.6	-0.4	-0.8	-13.3	-13	-13.5	-11.3	-2	-2.4	-15.2	-14.7	-15.5
II	-3.9	-0.8	1.5	-13.1	-15	-11.5	-9.9	-6.1	-2.1	-12.8	-14	-16.5
III	-5	-1.9	-1.5	-10.1	-14.5	-17.5	-9.9	-15	-5.2	-19.9	-24.2	-16.5
IV	-4.1	-2.4	0.2	-11.9	-9	-12.5	-8.9	-9	-7.5	-13	-13	-12.5
V	-1.2	0.1	-0.4	-12.9	-10	-11.5	-8.7	-6	-5.5	-12	-15	-15.5
VI	-3.3	-2	-1.1	-12.2	-14.4	-12.5	-9.4	-9	-1.8	-14.2	-16	-13.5
FSPL*	-19.7	-22	-38.5	-19.7	-22	-38.5	-19.7	-22	-38.5	-19.7	-22	-38.5

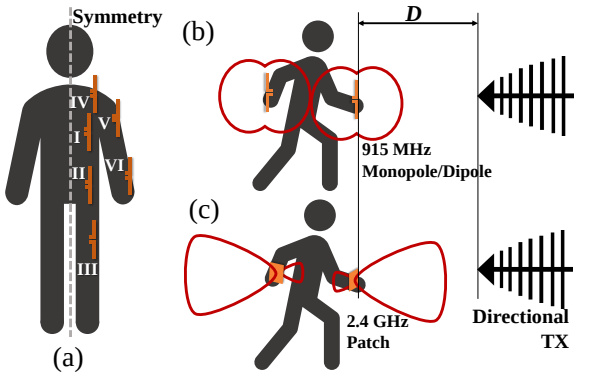

FIGURE 8. Measurement setup of indoor off-body propagation using the proposed antennas and a reference 915 MHz dipole antenna, horizontally-aligned, for distance D: (a) on-body antenna placement, (b) LOS and N-LOS scenarios for the omni-directional monopole, (c) LOS and N-LOS scenarios for the directional 2.4 GHz patch.

on the body. This is due to the improved isolation provided by the ground plane. However, it is still observed that the antenna's gain deteriorates by over 5 dB when measured at position VI at 3 cm clearance from the body. This shows significantly higher degradation compared to on-phantom measurements in an anechoic chamber reported in [23], where the radiation efficiency was reduced by less than 10% on the phantom.

On the other hand, when a N-LOS scenario is considered, the effective gain of the unshielded monopole is improved over a patch antenna. This is explained by the low back-radiation of the patch antenna, while this may be a figure of merit in directional WPT or communications, when the direction of incidence of the RF power is unknown, this implies that less energy will be received from the transmitter. The measured G_{eff} shows the same trend as the simulated off-body gain of the antennas, in Fig. 5, where the person (subject of measurements in Fig. 8) is different from the AustinMan model from [40]. Furthermore, when combining this with the overall lower propagation losses at 915 MHz, it can be concluded that WPT for BAN at sub-1 GHz bands enables a higher end-to-end efficiency. This will be validated through simulations of the RF-powered BAN in the next section.

V. WIRELESS POWER RECEPTION EVALUATION

As different on-body rectenna positions significantly affect the power received from an off-body source at the same distance, with up to 20 dB variation as shown in the empirical measurements using textile antennas on-body, multiple rectennas are to be placed on-body to improve the antennas' angular coverage. For both the 915 MHz monopole and the 2.4 GHz patch, four on-body antenna positions are considered. The antennas are positioned at points I, V from Fig. 8, on the model's chest and arm, at point IV (the model's shoulder) with the main beam directed above the user (X-direction in Fig. 5), and at point I on the model's back. The net radiation pattern of the four antennas, including mutual-coupling and body-shadowing effects, are combined in the 3D EM model to simplify the received power calculations. The textile rectennas are evaluated in two use-cases: a transmitter at the same height as the user (YZ plane), and a transmitter above the user (XY plane).

When simulating the network's performance using propagation models and the EIRP of a transmitter, the antenna's gain is often quoted as the main parameter [12], [26]. However, this neglects the impact of the 3D radiation patterns of the antenna. To illustrate, for non-stationary receivers, such as humans, the omni-directional gain of the antenna needs to be considered as alignment between the transmitter and receiver's main lobes is unlikely. This allows accurate prediction of the RFEH BAN's performance in LOS and N-LOS scenarios. The EM-simulated radiation properties of both antennas, and the measured textile antennas' effective gains are used to simulate the RF-powered BAN performance.

A. ANALYTICAL TRANSMITTER ANTENNA GAIN LIMIT

An additional parameter which can be utilized to optimize the RFEH BAN performance is the transmitter gain, where a higher gain antenna can be used to deliver the same EIRP output with a lower power output from the transmitter or the amplifier. Therefore, the end-to-end efficiency can be improved, due to transmitting at a lower power level. The transmitting antenna gain may then be utilized as a controllable parameter to improve the rectenna's power reception [12]. At 2.4 GHz and above, it is possible to increase the EIRP above 36 dBm by using a directional transmitter. However, for every 3 dB increase in the transmitter gain above 36 dBm the power input to the antenna needs to be reduced by 1 dB, up to 52 dBm.

By increasing the transmitting antenna's gain, the end-to-end efficiency in WPT can be improved at higher frequency bands such as the 5 GHz ISM-bands. Nevertheless, this is mostly limited to point-to-point WPT applications where the positions of the transmitter and receiver are fixed. In a wearable system, implementing directional narrow-beam WPT techniques will require complex control loops to ensure accurate beam-steering using a large transmitting phased array.

In practice, the physical size of the antenna limits the maximum achievable directivity and subsequently the gain. This can be estimated analytically using a simple loop antenna. A loop antenna is selected due to the availability of accurate closed-form expressions in literature to estimate the maximum gain based on the antenna's size [41].

Considering a simple loop antenna as an a example, the maximum directivity,

$$D = \frac{120\pi^2(ka)^2}{R}\max\{J^2[ka\sin(\theta)]\}, \qquad (2)$$

and subsequently the gain, is a direct function of the surface current J over the loop of radius a (2), where R is the radiation resistance, $k = 2\pi/\lambda$ is the wave constant, and θ is the angle at which the directivity is calculated [41]. A simple approximation to the solution of the integral has been proposed in [41] with a maximum error of 0.2 dB for both electrically small ($ka < \lambda/2$) and large ($ka > \lambda/2$) antennas.

Two loop antennas of radius a are considered to estimate the size requirements for a high gain transmitter for 915 MHz and 2.45 GHz WPT. The loops' peak gain has been calculated using the method in [41]. Fig. 9 shows the analytically-calculated directivity of the antennas as a function of their radius. It can be seen that to realize a transmitting antenna of high gain (over 9 dB) the antenna's radius becomes unrealistically-large for most IoT applications at 915 MHz. Thus, transmitters of higher gain than 10 dBi will not be considered in the RF-powered BAN simulations for practical antenna design considerations. It is important to note that although more innovative novel antenna designs and transmit-arrays can be employed to improve the transmitting gain without significantly increasing the size, high gain antennas typically require a large physical size (e.g. parabolic and horn antennas), even for aperture efficiencies exceeding 1 such as the textile patch in [23].

B. RF-POWERED BAN PERFORMANCE USING 3D ANTENNA GAIN

For a 3D space, the average gain of an ideal antenna is 0 dB regardless of the radiation pattern [39]. In [42], it was analytically demonstrated that a high-directivity antenna does not improve the received power from an ambient wave due to the variations in the propagation medium. However, [42] concludes that this may change for lower antenna efficiency. In this work, it is shown that a 915 MHz omnidirectional rectenna, with low radiation efficiency, can outperform its directional counterpart operating at 2.4 GHz when evaluated over meaningful 2D planes for body-worn energy harvesting.

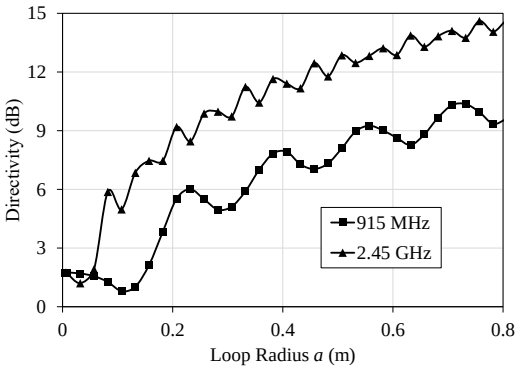

FIGURE 9. Loop antenna gain as a function of the radius at 915 MHz and 2.45 GHz.

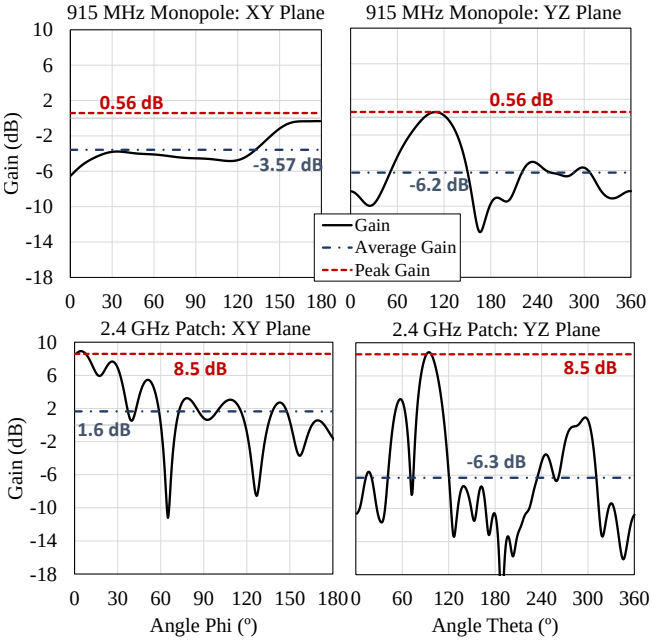

FIGURE 10. The patch and monopole antennas gain as a function of the angles theta (θ) and phi (ϕ), as well as the peak and average (mean) gains over each plane.

The angular gain of the entire receiving rectenna system, $G_{\mathrm{RX}}(\theta,\phi)$, is a function of the four rectennas placement in the 3D space around the body (x,y,z). The computed 3D patterns have been used to calculate the overall peak gain, the mean gains on the YZ and XY planes (planes defined in Fig. 5) as well as the angular gain to evaluate the performance of a randomly-aligned transmitter. Angles θ and ϕ are defined as the angular coordinates around the YZ and XY planes, defined in Fig. 5, respectively. Fig. 10 shows the Cartesian plot of the antennas' gain on the horizontal and vertical axis. The angular gain is directly influenced by the antennas' position on the body and can be used to evaluate the rectennas' performance in a 3D space (i.e. on the body)

$$G_{\mathrm{3D}}(x,y,z) \rightarrow G_{\mathrm{RX}}(\theta,\phi). \qquad (3)$$

Subsequently, the power received can be estimated using the angular-dependent gain to understand the performance of the BAN. Thus, the received RF power P_{RX} using free space propagation losses can be estimated including the angular dependency

$$P_{\mathrm{RX}}(x,y,z) = G_{\mathrm{RX}}(\theta,\phi)P_{\mathrm{TX}}\frac{1}{R^2}, \tag{4}$$

where R is the separation between the transmitter and the user and P_{TX} is the EIRP of the transmitter (4 W).

In order to demonstrate the variation in the simulated RFEH performance, three gain values are considered. The peak antenna gain $G_{\mathrm{Max.}} = \max\{G(\theta,\phi)\}$ is the most commonly utilized parameter in predicting the performance of RFEH and WPT networks [26]. The second metric is the average gain $G_{\mathrm{Avg.}}$, defined as the mean of the gain over the plane of interest, to account for the antenna's directionality. $G_{\mathrm{Avg.}}$ has been calculated independently for both θ and ϕ, and is shown in Fig. 10, using

$$G_{\mathrm{Avg:YZ}} = \frac{1}{360}\sum_{\theta=0}^{360^\circ} G(\theta), \tag{5}$$

$$G_{\mathrm{Avg:XY}} = \frac{1}{180}\sum_{\phi=0}^{180^\circ} G(\phi). \tag{6}$$

By considering the average gain rather than the peak gain, the performance of the rectenna when the receiving antenna's main lobe is not aligned with the transmitter can be accounted for, offering a more realistic insight on the antennas' performance. This work does not consider polarization mismatch; energy harvesting and WPT rectennas with dual-polarization reception capabilities have been widely presented based on dual-RF ports and dual-rectifiers with DC combining [43]. An extensive review of rectennas' polarization in RF energy harvesting and WPT applications has been presented in [11].

The average RF power received by the rectennas has been calculated using the free space propagation model and the antenna mean gains. A distance sweep has been carried out to show the spatial coverage range of an RF-powered BAN. The DC power is then calculated using the RF to DC Power Conversion Efficiency (PCE) of reported high-efficiency rectennas. The rectenna in [35] reports the highest sub-1 GHz PCE and is implemented on a flexible substrate using a dipole antenna, resulting in similar radiation properties to the textile monopole investigated in this work. At 2.4 GHz, the textile-based patch antenna coupled to a high efficiency rectifier in [23] achieves the highest PCE at power levels below -15 dBm. The measured and simulated PCEs from [35] and [23] are fitted to calculate the DC power output of the rectennas based on the textile antennas. Fig. 11 shows the measured and curve-fitted PCEs of the rectennas.

An EIRP of 4 W has been used when calculating the power delivered to the textile rectennas. The distance R between the transmitter and the rectenna has been swept from 2 m to 4 m. This ensures the rectenna is operating in the far-field, hence the path-loss model is valid. The rectenna's gain has been calculated using both the peak and mean gain obtained from the four antennas positioned on the body phantom, which is inclusive of the body shadowing effects, on-body propagation effects, and the mutual-coupling between the rectennas. Fig. 12 shows the calculated DC power received by the textile rectennas at 915 MHz and 2.4 GHz.

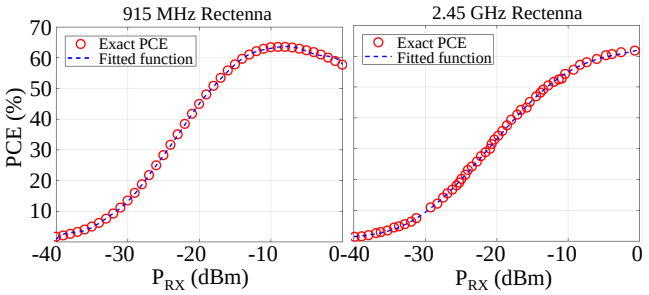

FIGURE 11. The flexible and wearable PCEs used at 915 MHz, [35], and 2.45 GHz, [23], to calculate the received DC power.

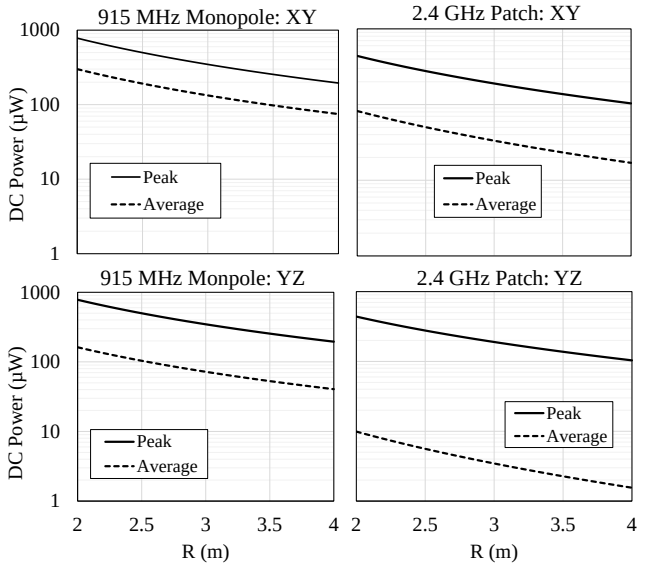

FIGURE 12. DC power received by the wearable 915 MHz and 2.4 GHz textile rectennas, on the XY and YZ planes, based on the antenna's peak and average (mean) gain.

One of the main aims of calculating the DC power delivered in a wireless-powered network is to evaluate the impact of certain antenna designs, based on the gain, on the power received by the rectennas. A higher DC power reception indicates a better BAN performance and a more suitable antenna design. The need to define multiple gain terms is clearly highlighted in Fig. 12, where the power delivered when considering the mean and maximum gains result in contradicting conclusions. When considering the antennas' peak gain, which is often quoted as the main figure-of-merit and assumes full angular alignment, the power received at 915 MHz is 0.77× higher than the power received at 2.4 GHz, on the XY plane. However, when considering the mean gainson the YZ and XY planes, the 915 MHz rectenna receives 15.4× and 2.6× higher DC power, respectively. This is

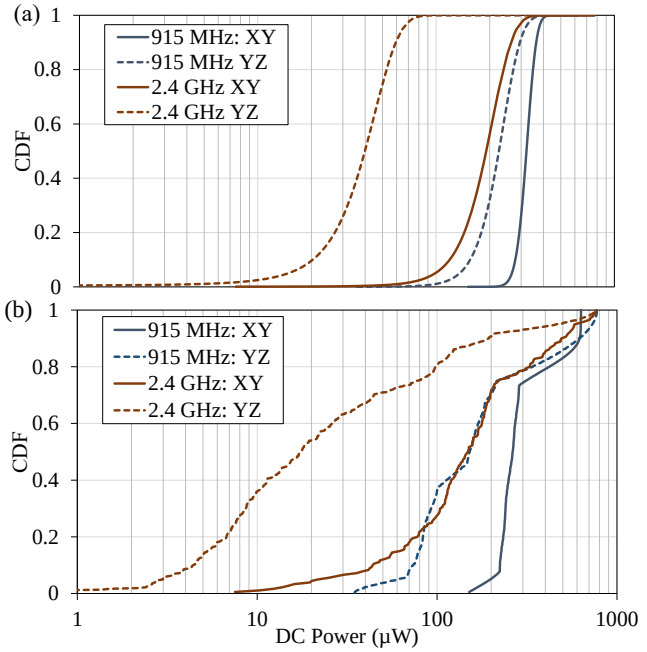

FIGURE 13. Theoretical (a) and empirical (b) CDF of the received DC power by the 915 MHz and 2.45 GHz rectennas.

despite the monopole having its efficiency and gain reduced due to the proximity with the human body model. Therefore, when delivering power to wearable rectennas, operating at a sub-1 GHz frequency using omnidirectional antennas yields higher DC power reception despite being more prone to body-shadowing and absorption. The difference in the received power ratio at both bands between the mean and peak gain is due to the significantly higher gain of the patch (6.84 dB) compared to the monopole (1.1 dB).

An additional optimization parameter for improving power reception in a BAN is the position of the transmitter with respect to the human. For both the 2.4 GHz and 915 MHz antennas, WPT from a source positioned above the user (on the XY plane of Fig. 5) results in improved energy reception. For a source above the user, such as mounted on the ceiling, the variation in the angular alignment of the antenna is limited to the 180° above the user. Subsequently, the average gain for both the broadside patch and the omnidirectional monopole on the XY plane is higher than on the YZ plane. In Fig. 12, at R=2 m on the YZ plane, the monopole antenna receives over eleven times higher DC power compared to the patch. The difference between the power received by both antennas is greater on the YZ plane due to the case where the transmitter is behind the user and not facing the radiating aperture of the patch antenna (the N-LOS scenario). This result agrees with the path loss measurements in table IV where the patch's effective gain is at its lowest in the N-LOS case and is lower than the monopole.

In real-life operation, the alignment of the rectenna with the power transmitter is random on the 360° YZ and 180° XY planes. Such random alignment is more prevalent when operating in the far fields of both the transmitter and the rectenna. Therefore, the probability of the received power needs to considered for both the XY and YZ axes. Fig. 13 shows the cumulative distribution function (CDF) of the received power at 2 m separation from the transmitter. From the CDF plots in Fig. 13, it is evident that the harvested power is higher when harvesting from the XY plane, for both the 915 MHz monopole and the 2.45 GHz patch. However, the effect us more prominent with the patch antenna, due to the more directional radiation patterns. Based on the empirical CDF in Fig. 13-b, the patch antenna's power reception CDF on the XY plane is comparable to the monopole. As a result, using a broadside patch antenna, positioned on the shoulder for instance, for harvesting from a source on the XY axis may result in improved energy reception compared to omnidirectional sub-1 GHz WPT. Nevertheless, it is concluded that on average and assuming a random position of the user, omnidirectional antennas combined with a source above the user (on the XY plane) result in the highest average received power, as in Fig. 12, as well as the highest power receiving probability, as in Fig. 13.

VI. CONCLUSION

In this paper, an RF-powered BAN with multiple power receivers, based on fully-textile antennas is studied, using realistic metrics for LOS and N-LOS dynamic WPT as opposed to peak gains. The effects of the frequency band, antenna design, and the antennas' position on the body have been investigated numerically and measured experimentally using textile antenna prototypes. Furthermore, more insightful real-world performance metrics are proposed improved RF-powered BAN evaluation.

Although omnidirectional sub-1 GHz textile antennas lack shielding from the body, the received DC power can be enhanced by over ten times compared to a 2.4 GHz high-gain patch antenna, when considering the average gain from a transmitter horizontally aligned with the body. The need for using the full 3D angular gain as well as the average gain when evaluating RF-powered networks is demonstrated, due to the random angular position of the user with respect to the power transmitter. The DC power reception improvement when using a 915 MHz monopole antenna has been quantified to vary between 0.7× and 15.4× higher DC power, depending on the plane of the incident RF power. It is concluded that omnidirectional sub-1 GHz antennas are the most suited for receiving power from an off-body source, when alignment between the user and the transmitter is unlikely and not controllable.

REFERENCES

[1] S. M. Salleh et al., "Textile Antenna With Simultaneous Frequency and Polarization Reconfiguration for WBAN," IEEE Access, vol. 6, pp. 2169–3536, 2018.

[2] M. Wagih, Y. Wei, and S. Beeby, "Flexible 2.4 GHz Sensor Node for Body Area Networks with a Compact High-Gain Planar Antenna," IEEE Antennas Wireless Propag. Lett., vol. 17, 12, pp. 49 – 53, 2018.

[3] S. Lemey, F. Declercq, and H. Rogier, "Textile Antennas as Hybrid Energy-Harvesting Platforms," Proceedings of the IEEE, vol. 102, no. 11, pp. 1833 – 1857, 2014.

[4] M. Wagih, A. Komolafe, and B. Zaghari, "Dual-Receiver Wearable 6.78 MHz Resonant Inductive Wireless Power Transfer Glove Using Embroidered Textile Coils," IEEE Access, vol. 8, pp. 24 630 – 24 642, 2020.

[5] X. Yang et al., "5G-Based User-Centric Sensing at C-Band," IEEE Trans. Ind. Informatics, vol. 15 no. 5, pp. 3040 – 3047, 2019.

[6] M. H. Rehmani et al., "IEEE Access special section editorial: Body area networks for interdisciplinary research," IEEE Access, vol. 4, pp. 2989– 2992, 2016.

[7] D. Balsamo et al., "Wearable and autonomous computing for future smart cities: open challenges," in 25th International Conference on Software, Telecommunications and Computer Networks (SoftCOM). IEEE, 2017, pp. 1–5.

[8] H. J. Visser and R. J. M. Vullers, "RF Energy Harvesting and Transport for Wireless Sensor Network Applications: Principles and Requirements," Proceedings of the IEEE, vol. 101, 6, pp. 1410 – 1423, 2013.

[9] O. B. Akan et al., "Internet of hybrid energy harvesting things," IEEE J. Internet of Things, vol. 5 no. 2, pp. 736 – 746, 2018.

[10] G. Monti, L. Corchia, and L. Tarricone, "UHF Wearable Rectenna on Textile Materials," IEEE Trans. Antennas. Propag., vol. 61, 7, pp. 3869 – 3873, 2013.

[11] M. Wagih, A. S. Weddell, and S. Beeby, "Rectennas for RF Energy Harvesting and Wireless Power Transfer: a Review of Antenna Design," IEEE Antennas and Propagation Magazine, vol. Accepted: In Press, 2019.

[12] O. Cetinkaya and G. Merrett, "Efficient deployment of UAV-powered sensors for optimal coverage and connectivity," in EEE Wireless Communications and Networking Conference, 2020.

[13] S. Shen, C.-Y. Chiu, and R. D. Murch, "Multiport Pixel Rectenna for Ambient RF Energy Harvesting," IEEE Trans. Antennas Propag., vol. 66, 2, pp. 644 –656, 2018.

[14] X. Lu et al., "Wireless networks with rf energy harvesting: A contemporary survey," IEEE Communications Surveys & Tutorials, vol. 17, 2, pp. 757 – 789, 2015.

[15] T. D. P. Perera et al., "Simultaneous Wireless Information and Power Transfer (SWIPT): Recent Advances and Future Challenges," IEEE Communication Surveys and Tutorials, vol. 20, 1, pp. 264 – 302, 2018.

[16] F. Bolos et al., "RF Energy Harvesting From Multi-Tone and Digitally Modulated Signals," IEEE Trans. Microw. Theory Techn., vol. 64, no. 6, pp. 1918 – 1927, 2016.

[17] A. P. Sample et al., "Design of an RFID-Based Battery-Free Programmable Sensing Platform," IEEE Trans. on Instrumentation and Measurement, vol. 57 no. 11, pp. 2608 – 2615, 2008.

[18] A. N. Abdulfattah et al., "Performance analysis of mics-based rf wireless power transfer system for implantable medical devices," IEEE Access, vol. 7, pp. 11 775 – 11 784, 2019.

[19] S. M. Asif et al., "A wide-band tissue numerical model for deeply implantable antennas for rf-powered leadless pacemakers," IEEE Access, vol. 7, pp. 31 031 – 31 042, 2019.

[20] K. N. Paracha et al., "Wearable Antennas: A Review of Materials, Structures, and Innovative Features for Autonomous Communication and Sensing," IEEE Access, vol. 7, 2019.

[21] M. Wagih, A. S. Weddell, and S. Beeby, "Millimeter-Wave Textile Antenna for On-Body RF Energy Harvesting in Future 5G Networks," in 2019 IEEE Wireless Power Transfer Conference (WPTC), 2019.

[22] D. Vital, S. Bhardwaj, and J. L. Volakis, "Textile Based Large Area RF-Power Harvesting System for Wearable Applications," IEEE Trans. Antennas Propag., vol. Early Access, 2019.

[23] S.-E. Adami et al., "A Flexible 2.45-GHz Power Harvesting Wristband With Net System Output From -24.3 dBm of RF Power," IEEE Trans. Microw. Theory Techn., 2018.

[24] M. Wagih, A. S. Weddell, and S. Beeby, "Sub-1 GHz Flexible Concealed Rectenna Yarn for High-Efficiency Wireless-Powered Electronic Textiles," in 2020 European Conference on Antennas and Propagation (EuCAP), 2020.

[25] J. A. E. and, "An RF-Harvesting Tightly-Coupled Rectenna Array Tee-Shirt with Greater than Octave Bandwidth," IEEE Trans. Microw. Theory Techniq., vol. Early Access, pp. 1 – 1, 2020.

[26] O. Cetinkaya et al., "Energy-Neutral Wireless-Powered Networks," IEEE Wireless Communications Letters, vol. 8 no. 5, pp. 1373 – 1376, 2019.

[27] T. A. Khan, A. Alkhateeb, and R. W. Heath, "Millimeter wave energy harvesting," IEEE Transactions on Wireless Communications, vol. 15, 9, pp. 6048 – 6062, 2016.

[28] M. Mozaffari et al., "Efficient Deployment of Multiple Unmanned Aerial Vehicles for Optimal Wireless Coverage," IEEE Communications Letters, vol. 20 no. 8, pp. 1647 – 1650, 2016.

[29] S. He et al., "Energy Provisioning in Wireless Rechargeable Sensor Networks," IEEE Transactions on Mobile Computing, vol. 12 no. 10, pp. 1931 – 1942, 2013.

[30] Y.-S. Chen, F.-P. Lai, and J.-W. You, "Analysis of Antenna Radiation Characteristics Using a Hybrid Ray Tracing Algorithm for Indoor WiFi Energy-Harvesting Rectennas," IEEE Access, vol. 7, pp. 38 833 – 38 846, 2019.

[31] T. Q. V. Hoang et al., "3D Voltage Pattern Measurement of a 2.45 GHz Rectenna," IEEE Trans. Antennas Propag., vol. 61, 6, pp. 3354 – 3356, 2013.

[32] A. Thielens et al., "A Comparative Study of On-Body Radio-Frequency Links in the 420 MHz–2.4 GHz Range," Sensors, vol. 18, 2018.

[33] A. R. Guraliuc et al., "Effect of textile on the propagation along the body at 60 ghz," IEEE Trans. Antennas Propag., vol. 62, 3, pp. 1489 – 1494, 2014.

[34] C. Kissi et al., "Directive Low-Band UWB Antenna for In-body Medical Communications," IEEE Access, vol. 7, pp. 149 026 – 149 038, 2019.

[35] M. Wagih, A. S. Weddell, and S. Beeby, "High-Efficiency Sub-1 GHz Flexible Compact Rectenna based on Parametric Antenna-Rectifier Co-Design," in 2020 IEEE MTT-S International Microwave Symposium, 2020.

[36] P. Nepa and H. Rogier, "Wearable Antennas for Off-Body Radio Links at VHF and UHF Bands: Challenges, the state of the art, and future trends below 1 GHz," IEEE Antennas and Propagation Magazine, vol. 57 no. 5, pp. 30 – 52, 2015.

[37] D. L. Paul et al., "Impact of Body and Clothing on a Wearable Textile Dual Band Antenna at Digital Television and Wireless Communications Bands," IEEE Trans. Antennas Propag., vol. 61 no. 4, pp. 2188 – 2194, 2013.

[38] K. W. Lui, O. H. Murphy, and C. Toumazou, "A Wearable Wideband Circularly Polarized Textile Antenna for Effective Power Transmission on a Wirelessly-Powered Sensor Platform," IEEE Trans. Antennas Propag., vol. 61 no. 7, pp. 3873 – 3876, 2013.

[39] C. A. Balanis, Antenna Theory: Analysis and Design.

[40] J. W. Massey and A. E. Yilmaz, "AustinMan and AustinWoman: High-fidelity, anatomical voxel models developed from the VHP color images," in 2016 38th Annual International Conference of the IEEE Engineering in Medicine and Biology Society (EMBC), 2016.

[41] H. Schrank and J. Mahony, "Approximations to the radiation resistance and directivity of circular-loop antennas," IEEE Antennas and Propagation Magazine, vol. 36 no 4, pp. 52 – 55, 1994.

[42] S. Shen et al., "An ambient rf energy harvesting system where the number of antenna ports is dependent on frequency," IEEE Trans. Microw. Theory Techn., vol. Early Access, pp. 1 – 12, 2019.

[43] H. Sun and W. Geyi, "A new rectenna with all-polarization-receiving capability for wireless power transmission," IEEE Antennas Wireless Propag. Lett., vol. 15, pp. 814 – 817, 2015.

MAHMOUD WAGIH (GS'18) received his B.Eng. (Hons) from the University of Southampton in 2018, where he is currently pursuing his PhD.

In 2017 he worked as a Research Assistant at the University of Southampton, supported by Intel, investigating novel transmission lines. He was an Intern in 2018 at Arm, UK, and currently at Arm Research. His current research interests lie in RF energy harvesting, wireless power transfer, wearable antennas, micro-power management and wireless sensor networks. He has over 20 journal and conference publications on these topics.

Mr. Wagih was the recipient of the Best Undergraduate Project Prize at the University of Southampton, 2018, and was selected for the IEEE MTT-S IMS Project Connect, 2019. He is the recipient of the Best Student Paper Award (First Prize) at the IEEE Wireless Power Transfer Conference 2019, and the Best Oral Paper Award at PowerMEMS 2019. He is a reviewer for 2 IEEE journals.

OKTAY CETINKAYA (S'13, M'18) received his B.Eng. degrees (Hons.) with a double major in Electrical Engineering & Electronics and Communication Engineering from Yildiz Technical University, Istanbul, Turkey, in 2013 and 2014, respectively. He then received his Ph.D. in Electrical and Electronics Engineering from Koc University, Istanbul, Turkey, in 2018.

He worked as a Research Fellow at the University of Southampton after his Ph.D. Since April 2020, he is a Research Associate at the University of Sheffield. His research interests broadly cover energy harvesting-aided wireless-powered communications for the Internet of Things, on which he published around 25 scientific papers in highly-respected journals and conference proceedings.

BAHAREH ZAGHARI received M.Sc degree (Hons) in Electromechanical Engineering in 2012 from the University of Southampton, U.K. She received her PhD in Dynamic analysis of a nonlinear parametrically excited system using electromagnets from Institute of Sound and Vibration (ISVR) at the University of Southampton in 2017.

Currently she is a Research Fellow at the school of Electronics and Computer Science, and she is working on the design of smart systems, such as the next generation of jet engines and smart cities. She has industrial, consultancy, and research experience in energy harvesting and instrumentation and has authored over 20 papers in the area.

Dr. Zaghari has received several awards for her outstanding performance in supporting women in academia.

ALEX S. WEDDELL (GS'06-M'10) received the M.Eng. degree (1st class honors) and Ph.D. in electronic engineering from the University of Southampton, U.K., in 2005 and 2010.

His main research focus is in the areas of energy harvesting and energy management for future Internet of Things devices. He has over 14 years' experience in design and deployment of energy harvesting systems, and has published around 55 peer-reviewed papers in the area. He is currently a Lecturer in the Center for Internet of Things and Pervasive Systems at the University of Southampton, and is involved with three projects funded by EPSRC, EU Horizon 2020 and Clean Sky 2.

STEVE BEEBY received the B.Eng. (Hons.) degree in mechanical engineering from the University of Portsmouth, Portsmouth, U.K., in 1992, and the Ph.D. degree in MEMS resonant sensors from the University of Southampton, Southampton, U.K., in 1998.

He was a Principal or Co-Investigator on an additional 18 projects and has coordinated two European Union research projects. He is currently the Head of the Smart Electronic Materials and Systems Research Group. He leads the U.K.'s Energy Harvesting Network. He is currently leading three U.K. funded research projects. He is a Co-Founder of Perpetuum Ltd., a University spin-out based upon vibration energy harvesting formed in 2004, Smart Fabric Inks Ltd., and D4 Technology Ltd. He has co-authored/edited four books including Energy Harvesting for Autonomous Systems (Artech House, 2010). He has given 17 invited talks and has over 250 publications and 10 patents. He has an h-Index of 50. His current research interests include energy harvesting, etextiles, MEMS, and active printed materials development.

Prof. Beeby was the recipient of two prestigious EPSRC Research Fellowships to investigate the combination of screen-printed active materials with micromachined structures and textiles for energy harvesting and was also awarded a Personal Chair in 2011. He is currently the Chair of the International Steering Committee for the PowerMEMS Conference series.